Available online at www.sciencedirect.com
ScienceDirect
Journal of Molecular Catalysis A: Chemical 272 (2007) 108–117
JOURNAL OF MOLECULAR CATALYSIS A: CHEMICAL
www.elsevier.com/locate/molcata

Effects of porphyrin composition on the activity and selectivity of the iron(III) porphyrin catalysts for the epoxidation of cyclooctene by hydrogen peroxide

Ned A. Stephenson, Alexis T. Bell *

Chemical Sciences Division, Lawrence Berkeley Laboratory, Department of Chemical Engineering, University of California, 201 Gilman Hall, Berkeley, CA 94720-1462, United States

Received 30 January 2007; received in revised form 8 March 2007; accepted 9 March 2007
Available online 15 March 2007

Abstract

A detailed investigation was carried out of the effects of porphyrin composition on the activity and selectivity of iron(III) porphyrin catalysts used for the epoxidation of cyclooctene by hydrogen peroxide. Under conditions where the formation of μ-oxo-dimers can be avoided, the mechanism of cyclooctene epoxidation and hydrogen peroxide decomposition are identical for all of the porphyrin catalysts investigated. It is observed that as the electron-withdrawing character of the phenyl groups is enhanced through halogenation, the tendency of iron(III) porphyrin chloride to dissociate decreases, but the Lewis acidity of the resulting iron(III) porphyrin cation increases. Increasing the Lewis acidity of the Fe(III) center also enhances the rate of heterolytic versus homolytic cleavage of the O–O bond of coordinated hydrogen peroxide, as well as the rate hydrogen peroxide consumption for olefin epoxidation versus peroxide decomposition. We have also shown that solvent composition affects both the extent of hydrogen peroxide coordination to the iron(III) porphyrin cation, thus affecting its activity, and the reactivity of hydrogen peroxide with the iron(IV) pi-radical cation, thus affecting the selectivity with which hydrogen peroxide is used for epoxidation.

Keywords: Porphyrin; Peroxide; Epoxidation; Mechanism; Cyclooctene

1. Introduction

Work carried out by Groves et al. at the end of the 1970s showed that iron(III) [tetraphenyl]porphyrin chloride, (TPP)FeCl, catalyzes the epoxidation of olefins by iodosylbenzene [1]. However, attempts to use this catalyst for olefin epoxidation with hydrogen peroxide as the oxidant have not been as successful, since (TPP)FeCl is not very selective [2–5] and is highly susceptible to degradation [4,5]. These observations have motivated the synthesis and evaluation of a large variety of porphyrin analogues in an attempt to improve the catalytic activity and robustness of porphyrin catalysts for use with hydrogen peroxide; reviews of this work are given in Refs. [6–9]. Most notable are the so-called second and third generation catalysts [5,10–14]. Second-generation analogues of (TPP)FeCl have substituents, usually halogens, on the phenyl groups attached to the *meso*-position of the porphyrin ring, whereas third-generation porphyrins have halogen atoms at the β-pyrrole positions on the porphyrin ring [10,11]. Halogenation of the phenyl groups has resulted in catalysts that are more selective for epoxidation over peroxide decomposition [5,9] and are less susceptible to degradation of the porphyrin ring [4,5]. Third-generation porphyrins, which contain halogen atoms at the β-pyrrole positions cause severe distortion of the porphyrin ring [9] and, as a result, reactivity studies have revealed that these catalysts are less robust [5] and less efficient [11] than second-generation iron porphyrins.

The selectivity of hydrogen peroxide for olefin epoxidation versus peroxide decomposition is determined by two competing reactions—heterolytic and homolytic cleavage of the oxygen–oxygen bond of hydrogen peroxide coordinated to the iron(III) cation [3,15]. Heterolytic cleavage of this bond leads to the formation of an iron(IV)-oxo pi-radical cation, which is an intermediate in hydrocarbon oxidation, whereas homolytic cleavage leads exclusively to peroxide decomposition [3,15]. It has also been reported that the high valent, iron-oxo pi-radical

* Corresponding author. Tel.: +1 510 642 1536; fax: +1 510 642 4778.
E-mail address: alexbell@berkeley.edu (A.T. Bell).

1381-1169/$ – see front matter © 2007 Elsevier B.V. All rights reserved.
doi:10.1016/j.molcata.2007.03.030

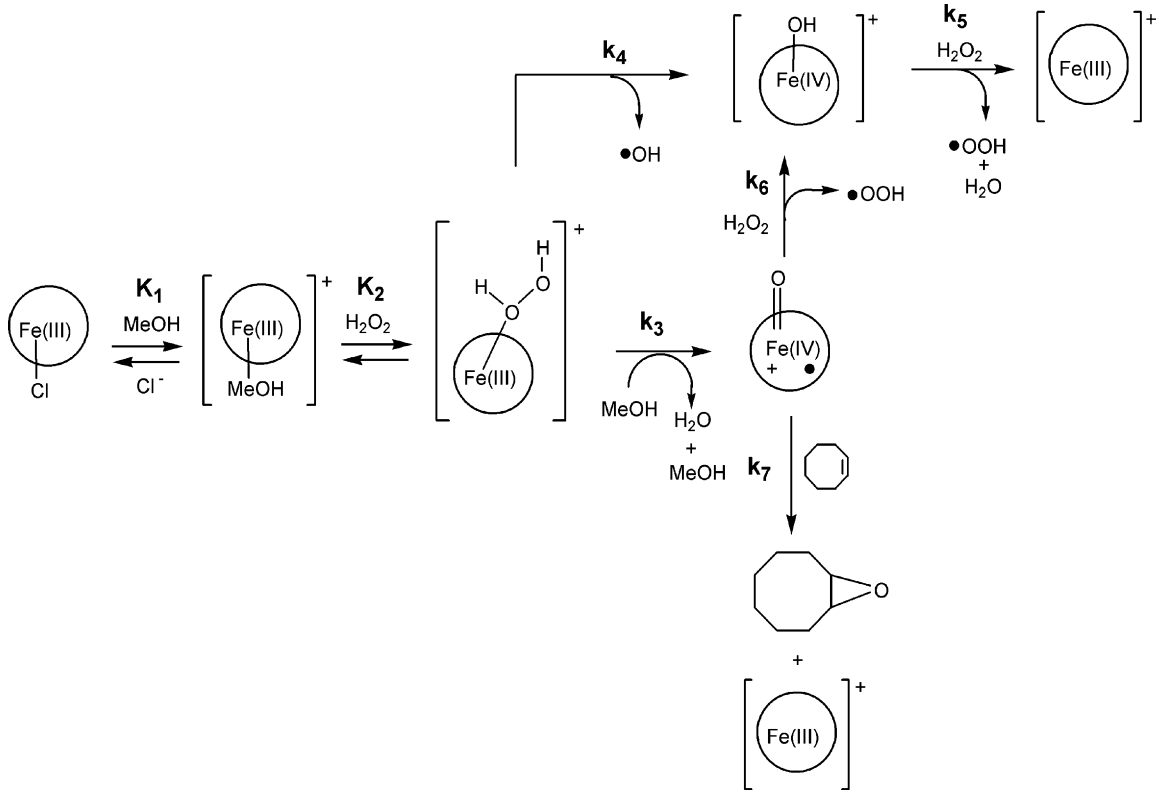

Fig. 1. The proposed mechanism for iron(III) porphyrin catalyzed epoxidation of cyclooctene by H_2O_2 in a methanol containing solvent. Note that the methanol ligand is not shown after reaction (2) for the sake of clarity.

cationic species can react to form an intermediate that leads to further decomposition of hydrogen peroxide [15–17]. Studies by Nam et al. have shown that the composition of second generation porphyrins affects both the selectivity for homolytic versus heterolytic cleavage of the O–O bond of coordinated H_2O_2 [3], and the selectivity of the iron(IV)-oxo pi-radical cation for hydrocarbon oxidation versus peroxide degradation [17]. This work demonstrated qualitatively that the addition of electronegative substituents improves the selective utilization of hydrogen peroxide for hydrocarbon oxidation over peroxide decomposition, but did not provide a detailed analysis of the effects of porphyrin composition on the mechanism and kinetics of the elementary processes involved in olefin epoxidation and peroxide decomposition.

In previous studies of olefin epoxidation by hydrogen peroxide catalyzed by (F_{20}TPP)FeCl, the kinetics of epoxide formation and hydrogen peroxide consumption are described very accurately for a wide range of reaction conditions by rate expressions derived from the reaction mechanism shown in Fig. 1 [15,18–20]. This has enabled us to determine the effects of solvent composition and axial ligand composition on the rate and equilibrium coefficients associated with each of the elementary reactions appearing in the mechanism. The purpose of the work reported here is, first, to determine the effects of porphyrin composition on the mechanism shown in Fig. 1 and, second, to quantify the effects of the halogenation of the phenyl groups attached to the porphyrin ring on the individual rate and equilibrium parameters.

2. Experimental

2.1. Reagents

Deuterium oxide, 99.9%, was obtained from Cambridge Isotope Laboratories, Inc. *cis*-Cyclooctene, 95%, was obtained from Alfa-Aesar. Iron(III) [tetrakis(pentafluorophenyl)] porphyrin chloride (F_{20}TPP)FeCl and dodecane, 99+%, were obtained from Aldrich. Omni Solv dichloromethane, 99.96%, methanol, 99.98%, ACS grade chloroform, 99.8%, and hydrogen peroxide, 30%, were all obtained from EMD Chemicals. Iron(III) [tetraphenyl]porphyrin chloride (TPP)FeCl, iron(III) [tetrakis(4-fluorophenyl)] porphyrin chloride (2-F_4TPP)FeCl, iron(III) [tetrakis(2,6-difluorophenyl)] porphyrin chloride (2,6-F_8TPP)FeCl, iron(III) [tetrakis(3,5-difluorophenyl)] porphyrin chloride (3,5-F_8TPP)FeCl, and iron(III) tetrakis(2,6-dichlorophenyl)] porphyrin chloride (2,6-Cl_8TPP)FeCl, and the μ-oxo dimer of iron(III) [tetrakis(3,5-difluorophenyl)] porphyrin chloride (3,5-F_8TPP)Fe–O–Fe(3,5-F_8TPP) were obtained from Frontier Scientific. The structures and compositions of the iron porphyrins used in this study are presented in Fig. 2, together with their full name and the symbol used to identify the porphyrin.

2.2. Reactions

Prior to initiating a reaction, cyclooctene, solvent, and catalyst were mixed in a 5 mL reaction vial. The solvent

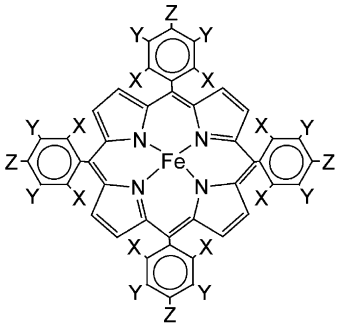

Porphyrin Catalyst	Symbol	X	Y	Z
iron (III) [tetrakisphenyl] porphyrin	(TPP)Fe	H	H	H
iron(III) [tetrakis(4-fluorophenyl)] porphyrin	(4-F_4TPP)Fe	H	H	F
iron(III) [tetrakis(2,6-difluorophenyl)] porphyrin	(2,6-F_8TPP)Fe	F	H	H
iron(III) [tetrakis(3,5-difluorophenyl)] porphyrin	(3,5-F_8TPP)Fe	H	F	H
iron(III) [tetrakis(pentafluorophenyl)] porphyrin	(F_{20}TPP)Fe	F	F	F
iron(III) [tetrakis(2,6-dichlorophenyl)] porphyrin	(2,6-Cl_8TPP)Fe	Cl	H	H

Fig. 2. Structure and terminology used for various iron(III) porphyrin catalysts.

consisted of a mixture of methanol and dichloromethane; the methanol concentration was 5.6 M unless specified otherwise. The cyclooctene concentration was varied depending on the experiment. The total reaction volume was held constant for all reactions at 3.35 mL by changing the concentration of dichloromethane. Reactions were initiated by addition of hydrogen peroxide (1–10 μL). To facilitate product analysis, 10 μL of dodecane was added as a standard to the reaction mixture. All reactions were performed at room temperature. Reactions using (TPP)FeCl as the catalyst were conducted under nitrogen using deoxygenated solvents since it was observed that the presence of oxygen promoted competitive reactions involving free-radicals. Evidence for radical oxidation was not observed for the other catalysts in the presence of air.

2.3. Product analysis

The concentration of cyclooctene epoxide as a function of time was determined by gas chromatography. Analysis was carried out using a HP 6890 Series gas chromatograph equipped with an Agilent DB Wax (30 m × 0.32 mm × 0.5 μm) capillary column and a FID detector. The temperature program for analysis was as follows: 2.5 min at 50 °C, ramp at 20 °C per min to 175 °C, and 1.5 min at 175 °C. The split/splitless inlet was operated at 200 °C and 14.2 psi with a split ratio of 5. Dodecane and cyclooctene epoxide were eluted at 5.5 and 8.2 min, respectively. The time required to analyze a single sample via gas chromatography was on the order of the time for the completion of the reaction. Therefore, multiple reactions were performed in order to obtain data points as a function of time and to verify reproducibility. The precision of measuring cyclooctene epoxide via gas chromatography was determined to be within ±1% by analysis of a calibrated standard.

2.4. Hydrogen peroxide consumption and analysis

The hydrogen peroxide concentration was measured as a function of time using ^{1}H NMR as described in Ref. [21]. These analyses were carried out using a 400 MHz VMX spectrometer. Samples were prepared in 5 mL reaction vials, as described above, with the exception that the catalyst was not added to the vial. A portion of this reaction mixture was transferred to a precision NMR tube. Chloroform was used as the internal standard. The reaction was initiated by adding a concentrated solution of porphyrin catalyst to the NMR tube prior to taking scans. A NMR spectrum was taken every 32 s by averaging the data from four scans. The area of the hydrogen peroxide peak, located at ∼10 ppm, was then integrated and compared to the area of an internal standard. ^{1}H NMR experiments were run in triplicate to verify the repeatability of the experiment.

Analysis of hydrogen peroxide in various solvents was carried out using a 400 MHz VMX spectrometer. ^{1}H NMR spectra were taken of the mixtures of hydrogen peroxide (14 mM) and solvent, which were prepared by adding 5 μL of standardized hydrogen peroxide solution to 3 mL of solvent.

2.5. Porphyrin analysis

Degradation of the porphyrin species was quantified by UV–vis spectroscopy using a Varian Cary 400 Bio UV–vis spectrometer. Scans of the reacting system were taken as a function of reaction time. The UV–vis spectra were then integrated to find the area under the peaks between 280 and 700 nm. An extinction coefficient was calculated based on a linear plot of integrated area versus porphyrin concentration. The repeatability of the UV–vis scans was shown to be better than ±2%. Negligible error was associated with taking repeated scans; all error was associated with the sample preparation.

Analyses of the porphyrin species were carried out using a 400 MHz VMX spectrometer to corroborate the exchange of the chloride ligand for a molecule of methanol. Additional experimental details for these ^{1}H NMR experiments can be found in Ref. [18].

3. Analysis of reaction kinetics

As noted in Section 1, our previous studies have shown that the kinetics of cyclooctene epoxidation by H_2O_2 catalyzed by (F_{20}TPP)FeCl are well described by rate expressions derived from the mechanism presented in Fig. 1 [15,18–20]. For the catalyst to become active (F_{20}TPP)FeCl must first dissociate into cations and anions (reaction (1)). Hydrogen peroxide then coordinates to the iron(III) cation (reaction (2)). The oxygen–oxygen bond of the iron(III)–hydrogen peroxide intermediate is then cleaved either heterolytically (reaction (3)) or homolytically (reaction (4)). Heterolytic cleavage results in the formation of iron(IV) pi-radical cation species which can either react further with hydrogen peroxide (reaction (6)) or epoxidize an olefin (reaction (7)). Homolytic cleavage results exclusively in peroxide decomposition via an iron(IV)-hydroxo intermediate. The mechanism presented in Fig. 1 can be used to derive Eqs. (1)–(4).

Here, k_{obs} is the observed rate coefficient for hydrogen peroxide consumption, k_3 and k_4 are the rate coefficients for Reactions (3) and (4) (see Fig. 1), and [Fe^{III}–MeOH] is the concentration of iron(III) methanol-coordinated porphyrin species.

$$\frac{d[H_2O_2]}{dt} = -k_{obs}[H_2O_2] \quad (1)$$

$$k_{obs} = \frac{k_3 K_2 [Fe^{III}\text{–MeOH}][MeOH]}{Y_\infty} \quad (2)$$

$$[H_2O_2] = [H_2O_2]_0 - \frac{[C_8\text{–O}]}{Y_\infty} \quad (3)$$

$$Y_\infty = \frac{[C_8\text{–O}]_\infty}{[H_2O_2]_0} \times 100\% \cong \frac{k_3\,[MeOH]}{k_3\,[MeOH] + 2k_4} \times 100\% \quad (4)$$

The value of k_{obs} was determined by measuring the initial rate of cyclooctene oxide production. This value was determined using Eq. (1), where k_{obs} is defined according to Eq. (2). Only methanol-coordinated porphyrin species, represented by Fe^{III}–MeOH in Eq. (2), are active catalytically [18,19]. The concentration of hydrogen peroxide is related to the concentration of cyclooctene oxide (C_8–O) via Eq. (3) using the final yield (Y_∞) of cyclooctene oxide. The assumption that the yield of epoxide is independent of the concentration of hydrogen peroxide was verified for each porphyrin catalyst. Since the yield and observed rate constants are independent of the concentration of hydrogen peroxide, the yield can be approximated according to Eq. (4) when reaction (6) does not contribute significantly to hydrogen peroxide consumption; here the yield is approximated as the ratio of the rate of peroxide consumption by heterolytic cleavage of the oxygen–oxygen bond of hydrogen peroxide to the sum of the rates of peroxide consumption by heterolytic and homolytic cleavage of the oxygen–oxygen bond of hydrogen peroxide. A factor of 2 is placed before the rate of homolytic cleavage, since two molecules of hydrogen peroxide are consumed via that reaction path (reactions (4) and (5)). It then follows that the values of k_3K_2 and k_4K_2 can be determined from k_{obs} and Y_∞. Values for all measured rate parameters are reported in Table 1.

The validity of determining the rate parameters exclusively from gas chromatography data was investigated by measuring the actual rates of hydrogen peroxide consumption via ^{1}H NMR. Rates of hydrogen peroxide consumption were measured both in the presence and absence of substrate. The individual rate parameters were determined by writing rate expressions for the mechanism shown in Fig. 1 and fitting the rate parameters to both the gas chromatography and ^{1}H NMR data. The values obtained for k_3K_2 and k_4K_2 using this method were within ±10% of those obtained using only the rate of cyclooctene oxide production as measured by gas chromatography. The rates of peroxide consumption were measured via ^{1}H NMR for all porphyrins except (F_{20}TPP)Fe, for which the rate of peroxide consumption was too rapid to allow for quantification by ^{1}H NMR.

The relative rates of reactions (6) and (7) were determined by measuring the yield of cyclooctene oxide as a function of the ratio of hydrogen peroxide to cyclooctene and then fitting the observed data by adjusting the ratio k_6/k_7. The fitted values of k_6/k_7 are given as the final entry in Table 1.

Table 1
Individual parameters determined from experimental data for various tetraphenyl iron porphyrins

Variable	(F_{20}TPP)Fe in MeCN, 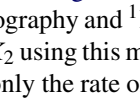	(F_{20}TPP)Fe in CH_2Cl_2, 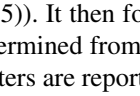	(TPP)Fe, 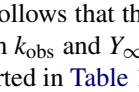	(2,6-Cl_8TPP)Fe, 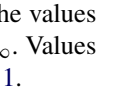	(2,6-F_8TPP)Fe, 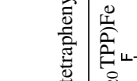	(3,5-F_8TPP)Fe, 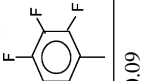	(4-F_4TPP)Fe, 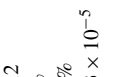
E_0 [Porp]FeCl (V)[a,b]		−0.09	−0.22	−0.25	−0.23	–	–
E_0 [Porp]Fe^+ (V)[c,d]		0.12	−0.11	−0.05	0.00	–	–
Porphyrin degradation	10%	3%	100%	56%	13%	100%	100%
Epoxide yield w.r.t. H_2O_2	88%	88%	45%	78%	88%	–	–
K_1	1.0×10^{-5}	1.3×10^{-5}	1.3×10^{-5}	60×10^{-5}	12×10^{-5}	0.4×10^{-5}	0.7×10^{-5}
[Fe–MeOH] (nM)	46	46	47	73	68	–	–
k_{obs} (min^{-1})	0.25	1.41	0.020	0.026	0.25	–	–
k_3K_2 ($M^{-2}\,s^{-1}$)	13	82	0.6	1.0	10	–	–
k_4K_2 ($M^{-1}\,s^{-1}$)	5.5	31	2.1	0.8	3.7	–	–
$k_3/k4$(M^{-1})	2.4	2.6	0.29	1.3	2.6	–	–
k_6/k_7	0.30	0.50	300	∼10	1.1	–	–

[a] Taken from Refs. [23,24].
[b] (TPP)FeCl in CH_2Cl_2 other porphyrins in 1:1 CH_2Cl_2:CH_3CN. All relative to SCE.
[c] Taken from Ref. [3] and converted from Fc/Fc^+ to SCE.
[d] Porphyrin cations formed by dissociation of chloride ligand in a 3:1 mixture of CH_3OH:CH_2Cl_2.

We have shown previously that the rate parameter k_5 can be determined by fitting hydrogen peroxide consumption rate data, determined via ^{1}H NMR, in the absence of olefin [15,22]. For k_5 to be determined by this technique, the rate of hydrogen peroxide consumption must be slow enough that the concentration of hydrogen peroxide can be determined temporally by ^{1}H NMR. In addition, k_5 must be less than $\sim 300\,M^{-1}\,s^{-1}$ or the contribution of reaction (5) to the rate of peroxide decomposition becomes indistinguishable from the overall rate of peroxide decomposition. In the present study, k_5 could not be determined for (F_{20}TPP)Cl because the rate of reaction was too rapid to be quantified by ^{1}H NMR, and values of k_5 for (TPP)FeCl, (2,6-F_8TPP)FeCl, and (2,6-Cl_8TPP)FeCl could not be determined because k_5 was sufficiently large that the contribution of reaction (5) could not be distinguished from the overall rate of peroxide decomposition.

4. Results and discussion

4.1. Aprotic solvent composition

In our previous studies of *cis*-cyclooctene epoxidation catalyzed by (F_{20}TPP)FeCl, a mixture of acetonitrile and alcohol was used as the solvent [15,19]. This solvent mixture could not be used for the present work, though, since all of the other porphyrins listed in Table 1 have limited solubilities in acetonitrile and methanol; however, all of these porphyrins are soluble in dichloromethane. Therefore, it was necessary to use a dichloromethane/methanol mixture instead of an acetonitrile/methanol mixture as the solvent. To determine whether the composition of the aprotic solvent affects the rate parameters, the experimental studies of (F_{20}TPP)FeCl reported previously [15,19], which had been carried out in an acetonitrile/methanol mixture, were repeated using a dichloromethane/methanol mixture. The concentration of oxidant, substrate, catalyst, and methanol were the same for experiments using both dichloromethane and acetonitrile, while equal volumes of aprotic solvents were used to maintain a constant reaction volume.

Initial studies of selectivity and reactivity under similar reaction conditions (0.72 M cyclooctene, 15 mM H_2O_2, 75 μM (F_{20}TPP)FeCl, 5.6 M methanol, 3.35 mL total volume) revealed that the selectivity for heterolytic cleavage is independent of the nature of the aprotic solvent, but that the rate of peroxide consumption is much faster in the presence of dichloromethane than in the presence of acetonitrile. As shown in Table 1, the observed rate constant for peroxide consumption was $1.4\,min^{-1}$ for the reaction carried out in dichloromethane/methanol and $0.25\,min^{-1}$ for the reaction carried out in acetonitrile/methanol. Additional experiments, similar to those carried out in acetonitrile/methanol, confirmed that the mechanism presented in Fig. 1 still applies when dichloromethane/methanol is used as the solvent.

Rate parameters for the reactions in dichloromethane/methanol, based on initial rate data, were determined and are compared in Table 1 to those obtained for reactions in acetonitrile/methanol. Several observations can be made. First, as expected from the proposed mechanism, the observed rate constant and yield of epoxide are independent of the initial concentration of hydrogen peroxide, verifying the pseudo first-order relationship expressed in Eq. (1). The equilibrium constant for reaction (1) was determined to be 1.3×10^{-5} via ^{1}H NMR. This value is slightly higher than that of 1.0×10^{-5} obtained for the acetonitrile/methanol system. To test the validity of this value, the observed rate constant was determined experimentally for varying porphyrin concentrations in the dichloromethane/methanol system. As shown in Fig. 3 and suggested by Eq. (2), k_{obs} is linearly related to the concentration of methanol-coordinated iron porphyrin as determined from the equilibrium constant K_1. In addition, the slope of the data in Fig. 3 predicts a value of $80\,M^{-2}\,s^{-1}$ for k_3K_2, which is similar to that obtained from the initial rate studies ($82\,M^{-2}\,s^{-1}$ as shown in Table 1).

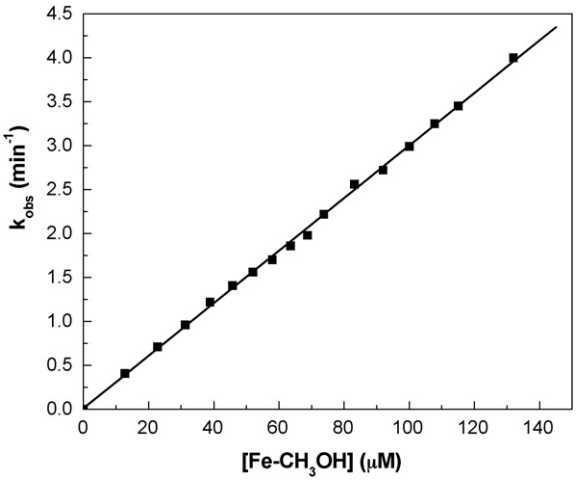

Fig. 3. Observed rate constant for (F_{20}TPP)Fe vs. the concentration of methanol-coordinated iron porphyrin as determined from $K_1 = 1.3 \times 10^{-5}$. The cyclooctene and hydrogen peroxide concentrations were 0.72 M and 16 μM, respectively, in a dichloromethane/methanol (3:1) solvent mixture.

As shown in Table 1, the rate parameters k_3K_2 and k_4K_2 are almost an order of magnitude greater when the epoxidation of cyclooctene is carried out in dichloromethane/methanol than when this reaction is carried out in acetonitrile/methanol. However, the ratios of k_3/k_4 are identical, indicating that k_3 and k_4 are independent of the composition of the aprotic solvent. Therefore, it follows that the difference in the observed rates of reaction is due primarily to a difference in the value of K_2 in dichloromethane versus acetonitrile. Two possibilities may explain the dependence of K_2 on the solvent composition. The first possibility is that hydrogen peroxide may compete with the solvent for coordination to the iron(III) cation. The second possibility is that solvent interactions with hydrogen peroxide may stabilize hydrogen peroxide in solution, and thereby, reduce its tendency to coordinate to iron porphyrin cations. The first of these options seems unlikely since hydrogen peroxide molecules are much more nucleophilic than any of the solvent molecules considered and are, therefore, expected to interact to a greater extent with the Lewis acidic iron(III) cation. Consistent with this, the observed rate of reaction is independent of the hydrogen peroxide concentration. If solvent molecules competed with

hydrogen peroxide for coordination to the iron(III) cation, then the observed rate of reaction would be expected to increase with increasing peroxide concentration.

The second explanation for the solvent dependence of K_2 seems more reasonable since hydrogen peroxide is expected to interact to varying degrees with different solvent molecules. Methanol, present in both sets of experiments, contains both a hydroxyl group and two lone pairs of electrons that can bond to hydrogen peroxide molecules. Acetonitrile also has a lone pair of electrons which can form a hydrogen bond with hydrogen peroxide molecules. On the other hand, dichloromethane does not have the ability to hydrogen bond with hydrogen peroxide. Hydrogen bonding between hydrogen peroxide and solvent molecules would affect the electronic properties of the hydrogen peroxide molecules and could consequently change the extent of coordination of hydrogen peroxide to the iron(III) cations. Evidence for the effects of the solvent on the electronic properties of hydrogen peroxide was obtained from ^{1}H NMR. For these experiments, spectra were taken of hydrogen peroxide (14 mM) in each solvent. The observed shifts of the hydrogen peroxide proton peak were 7.4, 9.3, and 11.3 ppm for dichloromethane, acetonitrile, and methanol, respectively. The greater extent of deshielding, as characterized by the downfield shift, indicates that the nucleophilicity of the hydrogen peroxide molecule decreases in the order of $CH_2Cl_2 > CH_3CN > CH_3OH$. A less nucleophilic hydrogen peroxide molecule would be expected to interact to a lesser extent with the Lewis acidic iron(III) cation. Therefore, the increased nucleophilicity of the hydrogen peroxide molecule in the presence of dichloromethane/methanol relative to acetonitrile/methanol explains the observed increase in the apparent equilibrium constant for reaction (2).

Experiments were also carried out to determine the effects of the methanol concentration on K_2. For these experiments, the total solvent volume was held constant at 3.0 mL while the relative amounts of methanol and dichloromethane were varied. As shown in Fig. 4, the observed rate constant increased to a maximum and then decreased. As seen in Eq. (2), k_{obs} is dependent on the concentration of methanol-coordinated porphyrin species, the concentration of methanol, and the yield, all of which increase with increasing methanol concentration. Inspection of Eqs. (2) and (4) leads to the expectation that k_{obs} should increase over the entire range of methanol concentration shown in Fig. 4. The observation that k_{obs} increases to a maximum and then decreases suggests that another parameter in Eq. (2) is affected by the relative concentrations of methanol and dichloromethane. As discussed in the previous paragraph, one possibility is that the equilibrium constant K_2 is affected by the solvent composition. As the methanol concentration increases, the extent of hydrogen bonding between hydrogen peroxide and methanol increases, decreasing the nucleophilicity of hydrogen peroxide and thereby reducing the value of K_2. Thus, the explicit dependence on methanol concentration resulting from Eqs. (2) and (4), which should lead to a monotonic increase in k_{obs}, is offset by the decrease in K_2 with increasing methanol concentration. The combined effects lead to a maximum observed rate constant near a methanol concentration of 10 M.

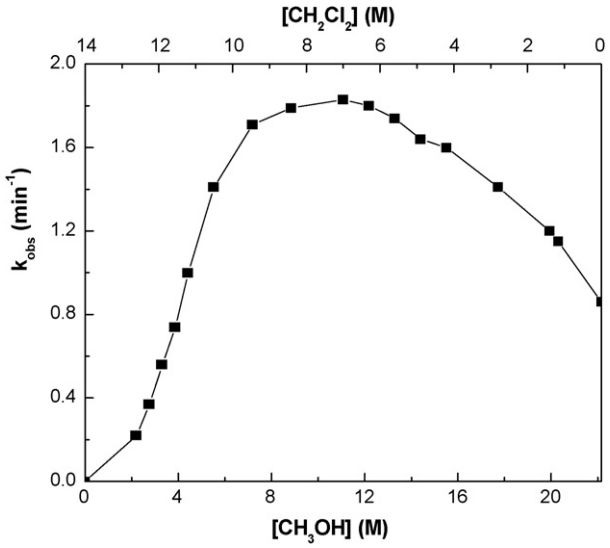

Fig. 4. The observed rate constant for (F_{20}TPP)Fe as a function of the methanol concentration. Cyclooctene, hydrogen peroxide, and porphyrin concentrations were 0.72 M, 16 mM, and 75 μM, respectively. Dichloromethane concentration varied to maintain constant volume.

There is reason to believe that the decrease of K_2 with increasing methanol concentration becomes significant only above 6 M. Fig. 5 shows that when k_{obs} is plotted versus the product of the methanol concentration and divided by the methanol-coordinated porphyrin concentration to the final yield a straight line is obtained with a slope equal k_3K_2. Linearity of the plot over the range of 0–6 M methanol indicates that K_2 is not affected significantly at low methanol concentrations. Note that the lower data points fall slightly below the best-fit line in Fig. 5; this is likely a result of underestimation of the observed rate constant due to excessive porphyrin degradation at low methanol concentrations.

The composition of the aprotic solvent was also observed to affect the competition between reactions (6) and (7) for the pi-radical cation species. The ratio of k_6/k_7 was determined to be 0.3

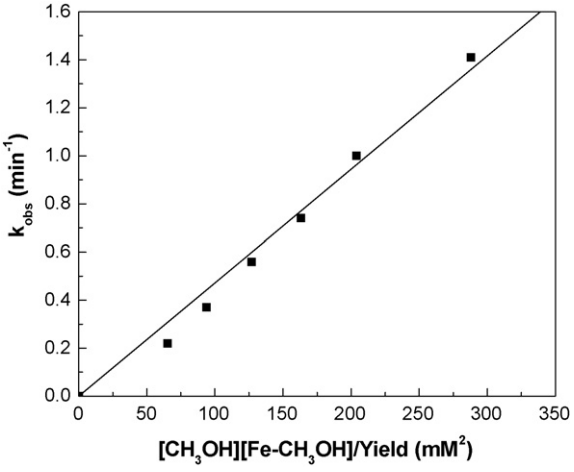

Fig. 5. Observed rate constant for (F_{20}TPP)Fe obeys Eq. (2) at low methanol concentrations. Cyclooctene, hydrogen peroxide, and porphyrin concentrations were 0.72 M, 16 mM, and 75 μM, respectively. Dichloromethane concentration varied to maintain constant volume.

in acetonitrile/methanol and 0.5 in dichloromethane/methanol. This observation can also be explained by the relative nucleophilicity of hydrogen peroxide in each of the solvent systems. The increase in the nucleophilicity of hydrogen peroxide in dichloromethane/methanol relative to acetonitrile/methanol makes it more reactive with the Lewis acidic pi-radical cation iron porphyrin species, thus increasing k_6/k_7.

4.2. Effects of phenyl group halogenation on the kinetics of cyclooctene epoxidation by iron porphyrins

Five other iron porphyrins (see Fig. 2) were studied in addition to (F_{20}TPP)FeCl. Numerous experiments were carried out in which porphyrin, hydrogen peroxide, and substrate concentration were varied in order to determine whether the epoxidation of cyclooctene using these catalysts follows the mechanism shown in Fig. 1. As will be discussed later, several of the porphyrin catalysts formed μ-oxo dimers as the porphyrin concentration was increased, resulting in a decreased yield of epoxide with increasing porphyrin concentration. To determine individual rate parameters independent of μ-oxo dimer formation for (TPP)FeCl, kinetic data were obtained at a low porphyrin concentration (75 μM). However, even at low porphyrin concentrations, μ-oxo dimerization occurred to a significant extent for (3,5-F_8TPP)FeCl and (4-F_4TPP)FeCl. Therefore, individual rate parameters were not determined for these catalysts. The epoxide yield for (2,6-Cl_8TPP)FeCl also decreased with increasing porphyrin concentration. Since it is well known that (2,6-Cl_8TPP)FeCl does not form μ-oxo dimers [25,26], another reaction pathway involving multiple equivalents of (2,6-Cl_8TPP)FeCl must contribute to the consumption of hydrogen peroxide at high porphyrin concentrations. To minimize the contribution of any such pathway, kinetic parameters were determined for (2,6-Cl_8TPP)FeCl at a low porphyrin concentration (25 μM). Additional details of the individual experiments for (TPP)FeCl, (2,6-Cl_8TPP)FeCl, (2,6-F_8TPP)FeCl, and (4-F_4TPP)FeCl are provided as supplemental information. The experimental data for (F_{20}TPP)FeCl and (2,6-F_8TPP)FeCl are consistent with the mechanism shown in Fig. 1 and the kinetics described by Eqs. (1)–(4) over the entire range of experimental conditions, while the data collected for (TPP)FeCl and (2,6-Cl_8TPP)FeCl are consistent with the mechanism at low porphyrin concentrations.

4.2.1. Influence of phenyl group composition on the dissociation of iron(III) porphyrin chloride

Using Eq. (5), the equilibrium constant, K_1, for the dissociation of the chloride ligand can be determined via ^{1}H NMR [18]. Methanol-coordinated and chloride-coordinated porphyrin species are represented by [Fe–MeOH] and [Fe–Cl], respectively. The value of K_1 (see Fig. 1) in a 1:3 methanol: dichloromethane mixture is given for each porphyrin catalyst in Table 1. For porphyrin catalysts resulting in the formation of μ-oxo dimers, the concentration of chloride anions in solution was calculated as the sum of the concentration of the methanol-coordinated porphyrin species and two times the concentration of the μ-oxo dimer species, based on the assumption that the chloride anions dissociate completely upon the formation of either species:

$$K_1 = \frac{[\text{Fe–MeOH}^+][\text{Cl}^-]}{[\text{Fe–Cl}][\text{MeOH}]} \quad (5)$$

As evidenced by a larger value of K_1, chloride dissociation from (TPP)FeCl becomes easier if halogen substituents are added to the *ortho*-positions of the phenyl groups, and chlorine substituents have a larger effect than do fluorine substituents. Previous research has noted a similar affect for the binding of *N*-methyl-imidizole to *ortho*-substituted porphyrins [14]. Those results and the present study suggest that size effects are more important than through-bond electronic effects. The increase in K_1 with increasing size of the *ortho*-halogen substituents is likely due to increased overlap of the electron clouds of the *ortho*-halogens with the pi-electron system of the porphyrin ring, resulting in electron donation toward the porphyrin ring. Increased electron donation back to the iron cation would be expected to decrease the Lewis acidity of the iron cation and hence weaken the iron–chloride bond [14]. The Fe^{3+}/Fe^{2+} reduction potential can be used as an indicator of the relative electronegativity of iron porphyrins; increased electronegativity of the porphyrin complex leads to a shift in the reduction potential to more positive values [3]. As seen in the first row of Table 1, the reduction potential of (2,6-Cl_8TPP)FeCl is more negative than (2,6-F_8TPP)FeCl, indicating that (2,6-Cl_8TPP)FeCl has a lower Lewis acidity and, hence, a weaker iron–chloride bond. While *ortho*-halogenation of tetra-aryl porphyrins promotes dissociation of the iron(III) porphyrin chloride salt, fluorine substituents on the *meta*- and *para*-positions decrease the value of K_1. Electronegative groups in the *meta*- and *para*-positions should result exclusively in electron withdrawal from the porphyrin ring, increasing the Lewis acidity of the iron cation, and thus increase the strength of the iron–chloride bond. As expected from increased electron-withdrawal, two fluorine substituents in the *meta*-positions make dissociation of the chloride ligand more difficult than does one fluorine substituent in the *para*-position.

(TPP)FeCl and (F_{20}TPP)FeCl dissociate to a similar extent. However, the values reported for the $Fe^{3+/2+}$ reduction potential in Table 1 are very different. This inconsistency can be explained by the fact that the reduction potential values taken from literature [23,24] were measured in different solvents. The reduction potential for (TPP)FeCl was measured in dichloromethane, while the reduction potentials of the other porphyrins were measured in a 1:1 mixture of dichloromethane and acetonitrile. Reduction potentials of porphyrins are known to be influenced by the solvent, and based on studies comparing solvent donor number and reduction potential of (TPP)FeX porphyrins, the $Fe^{3+/2+}$ reduction potential is expected to be approximately +0.1 V greater in acetonitrile than in dichloromethane [27–29]. This suggests that the reduction potentials for (TPP)FeCl and (F_{20}TPP)FeCl should be similar in the same solvent, thus explaining the similar extents of dissociation, which very likely result from offsetting effects between the electron donation of fluorine substituents in the *ortho*-position and the electron acceptance of fluorine substituents in the *meta*- and *para*-positions.

4.2.2. Effect of iron(III) porphyrin dissociation on the Lewis acidity of iron(III) porphyrin cations

It is evident from the reduction potentials reported in the first and second rows of Table 1 that the iron cation becomes more electronegative after the chloride anion dissociates. It is also noted that the reduction potential increases in the order of $(TPP)Fe^+ < (2,6\text{-}Cl_8TPP)Fe^+ < (2,6\text{-}F_8TPP)Fe^+ < F_{20}TPP)Fe^+$ once the chloride ligand is removed, indicating that the *ortho*-halogen substituents act as electron-donors when the chloride anion is coordinated and as electron-acceptors when chloride is dissociated. The change in function by the *ortho*-halogens may be a result of the structural conformation of the porphyrin, since porphyrin reduction potentials are affected by a combination of electronic and structural factors [30]. Chloride-coordination to the iron(III) cation causes the iron atom to be displaced out of the porphyrin plane, which affects the conformation and electronic nature of the porphyrin catalyst [31]. This structural change could increase the interaction between the electron clouds of the *ortho*-halogens and the pi-electron cloud of the porphyrin ring. Dissociation of the chloride ligand may allow the iron(III) cation to recede back into the porphyrin ring, which could reduce the extent of electron cloud overlap such that electron-withdrawing inductive effects dominate. Consistent with this idea, local density function calculations of free-base tetraphenyl porphyrins indicate that the *ortho*-halogens of both $(2,6\text{-}Cl_8TPP)^{2-}$ and $(2,6\text{-}F_8TPP)^{2-}$ exhibit electron-withdrawing effects, albeit to a lesser extent than *para*- or *meta*-substituents [32].

4.2.3. Effects of phenyl group composition on the relative rates of heterolytic versus homolytic cleavage of O–O bonds of the coordinated H_2O_2

Once a molecule of hydrogen peroxide has coordinated to the iron(III) porphyrin cation, the oxygen–oxygen bond of the coordinated hydrogen peroxide molecule can cleave either homolytically to create a one-electron oxidized iron(IV)-hydroxo species or heterolytically to create a two-electron oxidized iron(IV) pi-radical cationic species (see Fig. 1) [3,15]. Homolytic cleavage leads exclusively to peroxide decomposition, while the iron(IV) pi-radical cation created via heterolytic cleavage can either decompose hydrogen peroxide or epoxidize an olefin. Nam et al. have presented a qualitative model that shows that the cleavage of the oxygen–oxygen bond of the coordinated hydrogen peroxide molecule proceeds via both heterolytic and homolytic cleavage and that the ratio of heterolytic to homolytic cleavage increases as the electron-withdrawing ability of the porphyrin ligand increases [3].

As discussed above, all halogen substituents on the phenyl rings act as electron-withdrawing groups after dissociation of the chloride ligand. This pattern is observed by looking at the Fe^{3+}/Fe^{2+} reduction potential of the iron(III) porphyrin cation. A positive shift in the reduction potential is indicative of a more electron-deficient porphyrin complex and, hence, should increase the oxidation potential of the porphyrin macrocycle [3,30]. While the data in Table 1 do show, in general, that the selectivity towards heterolytic cleavage (k_3/k_4) increases with the reduction potential, the relationship between selectivity and the electronic properties of the porphyrin is much more complex. In particular, there is no difference in selectivity between $(F_{20}TPP)FeCl$ and $(2,6\text{-}F_8TPP)FeCl$ even though the former porphyrin is much more electronegative and exhibits a higher reduction potential. Therefore, the ratio of heterolytic to homolytic cleavage must also be affected by some other factor such as, for example, the conformation of the porphyrin ring. The size and position of the halogen substituents on the phenyl rings likely affects the angle between the phenyl plane and the porphyrin plane as well as the planarity of the porphyrin ring [33], a structural change which would be expected to affect the electronic properties of hydrogen peroxide coordinated to the iron cation. Since a molecule of alcohol is involved in the heterolytic cleavage of the oxygen–oxygen bond of hydrogen peroxide [19], changing the conformation of the porphyrin may also change the interaction of the coordinated hydrogen peroxide with the alcohol molecule facilitating heterolytic cleavage of the peroxide O–O, thus influencing the rate constant for reaction (3).

The absolute values for k_3K_2 and k_4K_2 are also shown in Table 1. The extent of interaction between the iron(III) cation and hydrogen peroxide is expected to increase as the iron(III) cation becomes more Lewis acidic, thus increasing K_2. The *meta*- and *para*-fluorines of $(F_{20}TPP)Fe^+$ are strongly electron withdrawing, which would be expected to increase K_2 and would explain in part the large values of k_3K_2 and k_4K_2 for $(F_{20}TPP)Fe$ relative to the other porphyrins. The orientation of the phenyl rings relative to the porphyrin plane and the degree of planarity of the porphyrin plane may also affect the extent of coordination of the hydrogen peroxide molecule to the iron(III) cation. However, the inability to isolate the hydrogen peroxide-coordinated porphyrin species makes it impossible to decouple the rate parameter K_2 from k_3 and k_4. Theoretical studies are needed to better understand the effects of the nature of the solvent, the electronic nature of the porphyrin, and the physical structure of the porphyrin on the coordination of hydrogen peroxide to the iron(III) porphyrin cation and the subsequent cleavage of the oxygen–oxygen bond. This would allow the rate parameter K_2 to be decoupled from the rate parameters for homolytic and heterolytic cleavage.

4.2.4. Effects of porphyrin composition on the selectivity of iron(IV) pi-radical cation species for cyclooctene epoxidation

H_2O_2 selectivity for epoxidation is determined by competition between hydrogen peroxide and olefin for reaction with the iron(IV) pi-radical cation, Reactions (6) and (7). As shown previously, increasing electron-donation from the axial ligand to the iron(IV) pi-radical cation species decreases the selectivity towards epoxidation [19]. Similarly, decreasing the electronegativity of the porphyrin ligand, as indicated by the reduction potential, decreases the rate of epoxidation (reaction (6)) relative to the rate of hydrogen peroxide decomposition (reaction (7)). This finding is consistent with the findings of Nam et al. [17]. Two reasons have been suggested to explain the increased selectivity towards epoxidation that occurs as electron density is withdrawn from the porphyrin ring. First,

iron(IV) pi-radical cations of electron-deficient porphyrins may exhibit a greater propensity for electron-transfer to an olefin than for hydrogen abstraction from a peroxide molecule [16]. Second, peroxide decomposition may be diffusion controlled while epoxidation is not [16]. Thus, increasing the electronegativity of the pi-radical cation would increase the rate of epoxidation but not the rate of peroxide decomposition, since it is diffusion controlled.

4.2.5. Porphyrin degradation

Degradation of the porphyrin catalyst is thought to occur via attack of the porphyrin ring by hydroxyl radicals [15,34]. Electron-withdrawing substituents increase the reduction potential of the porphyrin, thus protecting the catalyst from oxidative destruction [30]. Therefore, substitution of halogens for hydrogens on the phenyl ring should increase the robustness of the porphyrin catalyst. As seen in Table 1, an increase in the reduction potential does indeed reduce the catalyst's susceptibility to degradation.

4.2.6. Formation of μ-oxo dimmers

The mechanism shown in Fig. 1 suggests that the yield of epoxide should be independent of the porphyrin concentration. While this expectation was borne out for (F_{20}TPP)Fe and (2,6-F_8TPP)Fe, reactions carried out using (TPP)Fe, (3,5-F_8TPP)Fe, and (4-F_4TPP)Fe as catalyst showed a decrease in yield with increasing porphyrin concentration; see Fig. 6 for example. The results seen in this figure suggest that an additional mechanism, involving multiple equivalents of the porphyrin catalyst contributed to hydrogen peroxide decomposition when (TPP)Fe, (3,5-F_8TPP)Fe, or (4-F_4TPP)Fe was used as the catalyst. A possible explanation is that the porphyrins lacking halogen substituents at the *ortho*-positions of the phenyl groups form μ-oxo dimers, which are effective for catalyzing the decomposition of hydrogen peroxide but not for catalyzing the epoxidation of olefins.

The presence of a β-pyrrole resonance near 14 ppm in the ^{1}H NMR spectra of (3,5-F_8TPP)FeCl, (4-F_4TPP)FeCl, and (TPP)FeCl dissolved in methanol/dichloromethane confirmed that all three porphyrins do indeed form μ-oxo dimers [35,36]. It was also noted that the extent of dimerization increased in the order of (3,5-F_8TPP)FeCl > (4-F_4TPP)FeCl > (TPP)FeCl, indicating that dimerization occurs more readily for electronegative porphyrin species. The formation of μ-oxo dimers was minimal for low concentrations of (TPP)FeCl. Therefore, it was possible to make a meaningful comparison of the reactivity and selectivity of (TPP)FeCl to other iron porphyrin catalysts by obtaining kinetic data at low porphyrin concentrations. The details of these experiments and the subsequent data analysis are provided as supplemental information. On the other hand, the dimerization of (3,5-F_8TPP)FeCl and (4-F_4TPP)FeCl occurred to a significant extent, even at low porphyrin concentrations, making it impossible to carry out a similar study of kinetic activity for those two catalysts.

4.2.7. Catalytic activity of the μ-oxo dimmer

To understand the effects of μ-oxo dimers upon catalytic activity, a sample of the (3,5-F_8TPP) μ-oxo dimer was obtained and studied independently of the monomeric form. Analysis by ^{1}H NMR confirmed that only μ-oxo dimer species were present when dissolved in dichloromethane (see Fig. 7). Upon addition of methanol (5.6 M) to the sample, a second porphyrin species, characterized by a β-pyrrole peak at 82 ppm, was observed. This suggests that the formation of the μ-oxo dimer species is reversible. The peak location of the non-dimeric species is indicative of an iron porphyrin with a strongly bound axial ligand [35–38], most likely a hydroxo ligand. Hydroxo-coordinated porphyrins are well known to form μ-oxo dimers readily [36,39–41]. Also, as seen in Fig. 7, methanol-coordinated species, characterized by a peak near 55 ppm, are not formed by the interaction of the μ-oxo dimer with methanol. As shown previously, iron porphyrins with strongly bound axial ligands do not react with hydrogen peroxide [18,19,22,42,43]. Therefore, any observed reaction must result of reaction from the hydrogen peroxide with the μ-oxo dimer species. Reac-

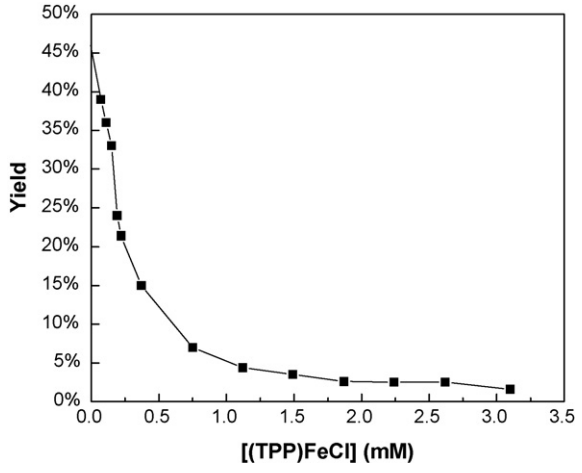

Fig. 6. Dependence of epoxide yield on total porphyrin concentration cyclooctene, hydrogen peroxide, and methanol concentrations were 3.8 M, 5.9 mM, and 5.6 M, respectively.

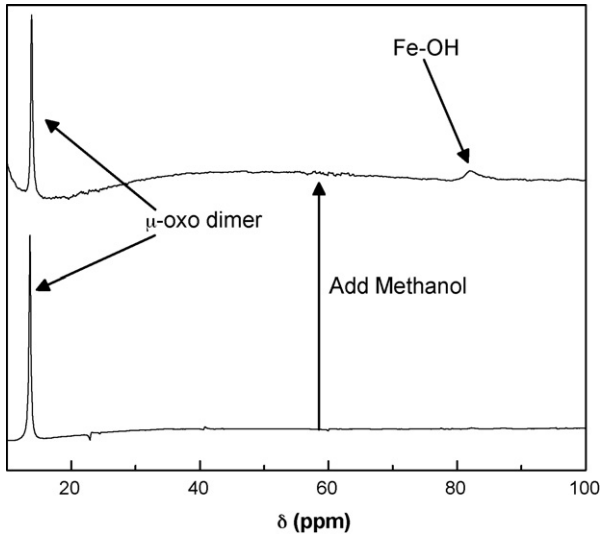

Fig. 7. ^{1}H NMR spectra of (3,5-F_8TPP)Fe–O–Fe(3,5-F_8TPP) before and after the addition of methanol (5.6 M).

tivity studies of the μ-oxo dimer of (3,5-F_8TPP)Fe in the presence of methanol revealed that the dimer decomposes hydrogen peroxide rapidly but is inefficient for the epoxidation of olefin. Therefore, the formation of the μ-oxo dimer when the monomeric (3,5-F_8TPP)FeCl is dissolved in methanol will result in reduced yields of epoxide. This is consistent with the proposal that the reduction in yield with increasing porphyrin concentration of (TPP)FeCl, (3,5-F_8TPP)FeCl, and (4-F_4TPP)FeCl is due to the formation of μ-oxo dimers.

5. Conclusions

The results of this study have shown that the composition of iron(III) porphyrins has a strong influence on the activity and selectivity of these materials for olefin epoxidation by hydrogen peroxide versus decomposition of hydrogen peroxide. The kinetics of olefin epoxidation and hydrogen peroxide decomposition are well described by the mechanism presented in Fig. 1 for all of the catalysts investigated (see Table 1) provided that conditions are avoided under which the porphyrin forms μ-oxo dimers. We find that the position and number of halogen atoms present on the phenyl groups bonded to the porphyrin affect the properties of the porphyrins in a number of ways. Increasing the electron-withdrawing character of the phenyl groups inhibits the dissociation of iron(III) porphyrin chloride (reaction (1)) but increases the Lewis acidity of the resulting iron(III) porphyrin cation and the extent of its coordination to hydrogen peroxide (reaction (2)). Higher electronegativity of the phenyl groups attached to the porphyrin ring also causes an increase in the ratio of the rate coefficients for reactions (3) and (4), as well as a decrease in the ratio of the rate coefficients for reactions (6) and (7). A rise the ratio of k_3 to k_4 is associated with an increase in the rate of heterolytic relative to homolytic cleavage of the O–O bond of coordinated hydrogen peroxide. Finally, we have shown, for the first time, that the extent of hydrogen peroxide coordination to the iron(III) cation in reaction (2) is affected significantly by the intermolecular interactions between the solvent and hydrogen peroxide molecules. As a result of these combined effects, the most electronegative porphyrin (F_{20}TPP)FeCl, dissolved in a methanol/dichloromethane solvent mixture, is found to be the most active and selective catalyst for the epoxidation of cyclooctene via hydrogen peroxide.

Acknowledgment

This work was supported by the Director, Office of Basic Energy Sciences, Chemical Sciences Division of the U.S. Department of Energy under Contract DE-AC02-05CH11231.

Appendix A. Supplementary data

Supplementary data associated with this article can be found, in the online version, at doi:10.1016/j.molcata.2007.03.030.

References

[1] J.T. Groves, T.E. Nemo, R.S. Myers, J. Am. Chem. Soc. 101 (1979) 1032–1033.
[2] W. Nam, S.Y. Oh, Y.J. Sun, J. Kim, W.K. Kim, S.K. Woo, W. Shin, J. Org. Chem. 68 (2003) 7903–7906.
[3] W. Nam, H. Han, S. Oh, Y.J. Lee, M. Choi, S. Han, C. Kim, S. Woo, W. Shin, J. Am. Chem. Soc. 122 (2000) 8677–8684.
[4] I.D. Cunningham, T.N. Danks, J.N. Hay, I. Hamerton, S. Gunathilagan, C. Jankczak, J. Mol. Catal. A: Chem. 185 (2002) 25–31.
[5] E. Porhiel, A. Bondon, J. Leroy, Tetraherdon Lett. 39 (1998) 4829–4830.
[6] D. Mansuy, Coord. Chem. Rev. 125 (1993) 129–141.
[7] D. Mansuy, Pure Appl. Chem. 59 (1987) 759–770.
[8] P.A. Adams, Preox. Chem. Biol. 2 (1991) 171–200.
[9] D. Dolphin, T.G. Traylor, L.Y. Xie, Acc. Chem. Res. 30 (1997) 251–259.
[10] R.A. Sheldon, Metalloporphyrins in Catalytic Oxidations, Marcel Dekker, New York, 1994.
[11] Z. Gross, L. Simkhovich, Tetrahedron Lett. 39 (1998) 8171–8174.
[12] A.A. Guedes, J.R.L. Smith, O.R. Nascimento, D.F.C. Guedes, M.D. Assis, J. Braz. Chem. Soc. 16 (2005) 835–843.
[13] E. Baciocchi, T. Boshci, L. Cassioli, C. Galli, A. Lapi, P. Tagliatesta, Tetrahedron Lett. 38 (1997) 7283–7286.
[14] R. Koerner, J.L. Wright, X.D. Ding, M.J.M. Nesset, K. Aubrecht, R.A. Watson, R.A. Barber, L.M. Mink, A.R. Tipton, C.J. Norvell, K. Skidmore, U. Simonis, F.A. Walker, Inorg. Chem. 37 (1998) 733–745.
[15] N.A. Stephenson, A.T. Bell, J. Am. Chem. Soc. 127 (2005) 8635–8643.
[16] T.D. Traylor, S. Tsuchiya, Y.S. Byun, C. Kim, J. Am. Chem. Soc. 115 (1993) 2775–2781.
[17] M.G. Yeong, W. Nam, Inorg. Chem. 38 (1999) 914–920.
[18] N.A. Stephenson, A.T. Bell, Inorg. Chem. 45 (2006) 5591–5599.
[19] N.A. Stephenson, A.T. Bell, Inorg. Chem. 45 (2006) 2758–2766.
[20] N.A. Stephenson, A.T. Bell, J. Mol. Catal. A 258 (2006) 231–235.
[21] N.A. Stephenson, A.T. Bell, Anal. Bioanal. Chem. 381 (2005) 1289–1293.
[22] N.A. Stephenson, A.T. Bell, Inorg. Chem. 46 (2007) 2278–2285.
[23] M.H. Lim, Y.J. Lee, Y.M. Goh, W. Nam, C. Kim, Bull. Chem. Soc. Jpn. 72 (1999) 707–713.
[24] J.E. Lyons, P.E. Ellis, H.K. Myers, J. Catal. 155 (1995) 59–73.
[25] B. Meunier, Biomimetic Oxidations Catalyzed by Transition Metal Complexes, Imperial College Press, London, 1999.
[26] P.S. Traylor, D. Dolphin, T.G. Traylor, J. Chem. Soc. Chem. Commun. (1984) 279–280.
[27] K.M. Kadish, J. Electroanal. Chem. 108 (1984) 261–274.
[28] P. O'Brien, D.A. Sweigart, Inorg. Chem. 24 (1985) 1405–1409.
[29] L.A. Bottomley, K.M. Kadish, Inorg. Chem. 20 (1981) 1348–1357.
[30] A. Ghosh, J. Am. Chem. Soc. 117 (1995) 4691–4699.
[31] M.S. Liao, S. Scheiner, J. Comput. Chem. 23 (2002) 1391–1403.
[32] A. Ghosh, J. Mol. Struct. (Theo.) 388 (1996) 359–363.
[33] A. Rosa, G. Ricciardi, E.J. Baerends, J. Phys. Chem. A 110 (2006) 5180–5190.
[34] I.D. Cunningham, T.N. Danks, J.N. Hay, I. Hamerton, S. Gunathilagan, Tetrahedron 57 (2001) 6847–6853.
[35] E.R. Birnbaum, J.A. Hodge, M.W. Grinstaff, W.P. Schaefer, L. Henling, J.A. Labinger, J.E. Bercaw, H.B. Gray, Inorg. Chem. 34 (1995) 3625–3632.
[36] R.J. Cheng, L. Latos-Grazynski, A.L. Balch, Inorg. Chem. 21 (1982) 2412–2418.
[37] T.C. Woon, A. Shirazi, T.C. Bruice, Inorg. Chem. 25 (1986) 3845–3846.
[38] J.T. Groves, R. Quinn, T.J. McMurry, M. Nakamura, G. Lang, B. Boso, J. Am. Chem. Soc. 107 (1985) 354–360.
[39] J.W. Buchler, Angew. Chem. Int. Ed. 17 (1978) 407–423.
[40] L. Fielding, G.R. Eaton, S.S. Eaton, Inorg. Chem. 24 (1985) 2309–2312.
[41] K.M. More, G.R. Eaton, S.S. Eaton, Inorg. Chem. 24 (1985) 3698–3702.
[42] W. Nam, M.H. Lim, S.Y. Oh, J.H. Lee, H.J. Lee, S.K. Woo, C. Kim, W. Shin, Angew. Chem. Int. Ed. 39 (2000) 3646–3649.
[43] W. Nam, H.J. Lee, S.Y. Oh, C. Kim, H.G. Jang, J. Inorg. Biochem. 80 (2000) 219–225.